

Article

An Experimental Study on the Cell Balancing Parameters for Faulty Cell Detection in a Battery Module

Woongchul Choi¹ and Sungsoo Hong^{2,*}¹ Department of Automotive Engineering, Kookmin University, Seoul 02707, Korea² Department of Electrical Engineering, Kookmin University, Seoul 02707, Korea

* Correspondence: hongss@kookmin.ac.kr

Abstract: Along with global efforts to reduce the carbon footprint, electrification of powertrains is occurring in various applications, certainly including transportation systems. One of the most important components is an electric energy storage system, i.e., a battery pack. Regardless of battery form factors, such as cylindrical, pouch and prismatic type, it is critical to maintain the safety of the battery module/pack by monitoring the conditions of each and every battery cell of the battery pack. It becomes even more critical as the battery cells are used over many charging and discharging cycles. Thermal runaways of the battery packs can even be triggered by a single faulty battery cell which degrades in an unexpected manner and speed compared to the neighboring battery cells, resulting in extreme fire hazards. Typically, this faulty cell with an abnormally increased internal resistance can be detected using a voltage sensor or a temperature sensor. However, in this study, instead of depending on those sensors, activities of cell balancing switching devices are used to identify a degraded cell compared to other cells in a relative manner. A currently proposed faulty cell detection algorithm was developed through multiple simulations with Matlab Simulink[®], then, a simple BMS prototype was built and tested as a proof of concept.



Citation: Choi, W.; Hong, S. An Experimental Study on the Cell Balancing Parameters for Faulty Cell Detection in a Battery Module.

Batteries **2022**, *8*, 218. <https://doi.org/10.3390/batteries8110218>

Academic Editors: Juan Carlos Álvarez Antón and David Anseán

Received: 10 September 2022

Accepted: 2 November 2022

Published: 5 November 2022

Publisher's Note: MDPI stays neutral with regard to jurisdictional claims in published maps and institutional affiliations.



Copyright: © 2022 by the authors. Licensee MDPI, Basel, Switzerland. This article is an open access article distributed under the terms and conditions of the Creative Commons Attribution (CC BY) license (<https://creativecommons.org/licenses/by/4.0/>).

Keywords: lithium-ion battery; battery module/pack; battery management system; passive cell balancing; faulty cell detection

1. Introduction

The development of lithium-based battery technology has attracted more and more attention due to the strong demands for green energy, and one of the main applications is the electrification of transportation using rechargeable lithium-ion batteries [1–4]. Along with the demand increase in battery cells for electric vehicle (EV) applications, yet another major market for batteries, energy storage systems (ESSs) for renewable energy generation is surely expected to grow solidly, where the ESS contributes to the regulation of generated electricity from irregular renewable energy generation devices [5,6], as green energy policies around the world will prevail eventually. Consequently, all these demands for energy storage systems have brought great opportunities for lithium-ion battery manufacturers and final application system manufactures and, at the same time, major challenges in regard to the safety of the battery systems. More specifically, as opportunities, battery modules and/or packs utilizing lithium-ion battery cells are considered to be an eco-friendly energy storage platform in various applications such as land and sea transportation systems, renewable energy distribution facilities and many more [2,4,7]. However, as one of the major challenges, huge liabilities are found be on battery cell manufacturers, battery pack system integrators and final product manufacturers, yet it is still hard to define the lines of responsibilities among them clearly. One of the most critical issues is the thermal runaway, which is near un-extinguishable in fire incidents. This fatal incident can be triggered by various reasons such as inherent cell defects from cell manufacturers, irregular cell aging among cells from the charging and discharging process of the application systems and

more. As a way to address this critical problem, a battery management system (BMS) is used for monitoring each and every battery cell in the system. The BMS maintains the battery cells within optimal conditions to ensure safety and issues warnings and alarms when it detects presets of dangerous conditions from any cell in the battery pack. As a result, the BMS is considered to be the most crucial element of the battery pack system in order to maximize the safety of the system by monitoring the battery status, such as voltages, currents and temperatures of every cell in real time [6–10]. There are many algorithms to detect various abnormalities of cell behaviors, especially the cell imbalances, as discussed in various research papers [9,10]. In the current research, a straightforward approach is proposed, as it requires near minimal resources and process time to detect faulty cells among neighboring cells. The idea was developed through simulations, and then, a concept-of-proof experiment was conducted to obtain the initial results.

2. Battery System Modeling for Development of Faulty Cell Detection Algorithm

2.1. Simulation of Battery Module with a Battery Management System

The simulation model was developed to mimic a three-cell lithium-ion battery module with a simple battery management system, as shown in Figure 1. In order to concentrate on the development of a faulty cell detection algorithm, a passive cell balancing function and an over-charging/over-discharging protection function were closely investigated.

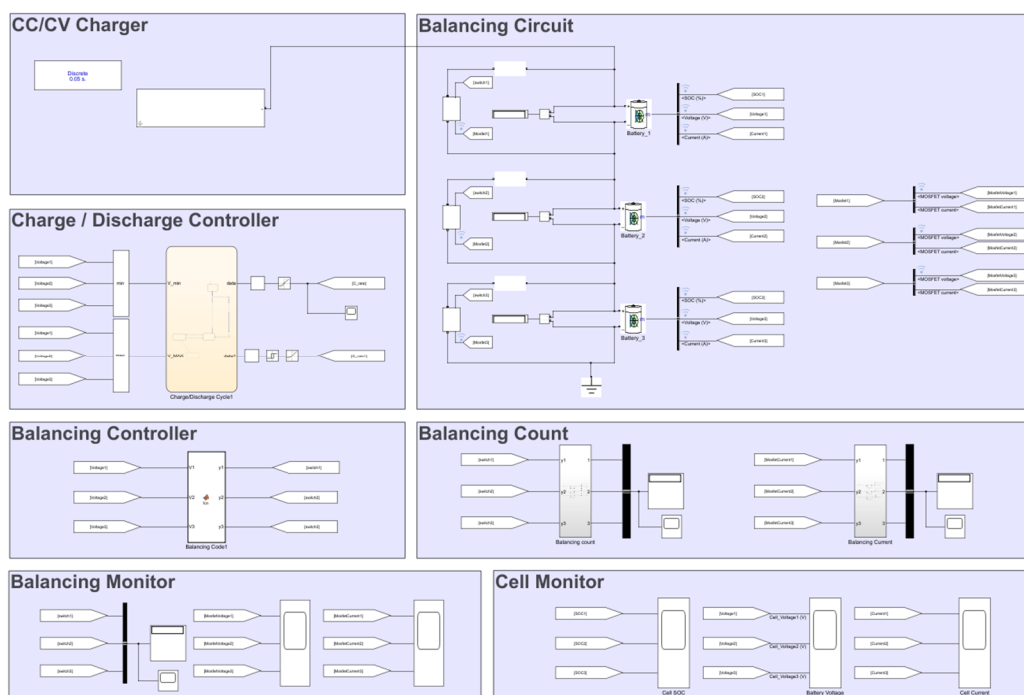


Figure 1. A model with a battery module and a battery management system.

The passive balancing process is one of the balancing techniques. The idea is to set a maximum voltage of the cells as an upper bound for the protection of the cells in the module. During the charging process, when a weak cell, typically with a higher internal resistance, reaches the upper bound, the BMS connects the weak cell to a resistor using an electronic switching device. By completing the energy dissipative circuit through the resistor, the cell voltage of the weak cell comes down to a safe level, allowing the charging process for all the cells to resume [11–14]. This seemingly simple technique is widely used in various applications due to its low cost and simplicity. In this study, the simulations were carried out using Matlab Simulink®, and the experiments were conducted focusing on the development of a faulty cell detection algorithm using a simple BMS without additional sensors.

2.2. Key Parameters of a Proposed Faulty Cell Detection Algorithm

In general, battery cells with an increased internal resistance and abnormally higher temperature due to any defects are detected using temperature sensors [15]. However, in the current study, a newly proposed algorithm detects a faulty cell within the module simply by counting the switching actions during the passive cell balancing process. One of the distinct features of a faulty cell is that the voltage rises faster than normal healthy cells during the charging process due to the increase in internal resistance, resulting in a shorter charging time than those of normal cells [16,17]. Based on this characteristic, the key parameters are selected, as shown in Table 1, and they are traced for each and every cell through the simulations and the proof-of-concept experiments. The balancing time is measured from a point when the first balancing initiates its switching action until the charging is complete. The balancing count is a number of switching device operations during the balancing process.

Table 1. Key parameters traced during balancing process.

Parameters	Unit
Balancing time	Second
Balancing count	Count

2.3. Battery Module Setup

The battery module consists of three cells in series for its simplicity. While the increase in parallel connections of cells reduces the impact on internal resistance relative to serial connections, the additional sensors to measure voltages and current imbalances between each cell in the module due to parallel connection characteristics increase the system cost [10]. Thus, the simulations and the corresponding experiments were prepared using the serial connection in which voltage imbalance is deepened, along with battery degradation. In order to mimic the different aging characteristics realistically, cell impedances are given differently based on measured values from actual battery cells, as shown in Table 2.

Table 2. Cell impedances for simulations.

Module 1	Impedance [mΩ]
Cell #1	0.0695
Cell #2	0.0716
Cell #3	0.0799

2.4. Simulation of Cell Balancing Process

A number of simulations of the dissipative cell balancing process were conducted following the flowchart displayed in Figure 2. The battery module specification used in the simulation is provided in Table 3. The simulations were carried out with a typical charging process, where 1 C-rate (2.6 A in the current setup) current was applied up to 12.6 V following the CC–CV (Constant Current–Constant Voltage) charging protocol. During charging, when the voltage reached its balancing voltage (4.2 V), the balancing processes were initiated and the time and the count of the switching device operations for each cell were traced, respectively.

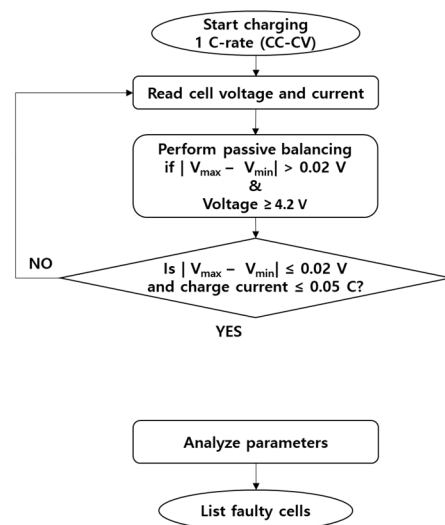


Figure 2. Flowchart of the algorithm.

Table 3. Battery module specification.

Specification	Value	Unit
Nominal voltage	11.1	V
Fully charged voltage	12.60	V
Fully discharged voltage	8.75	V
Rated capacity	2600	mAh
Charge cut-off voltage	12.75	V
Discharge cut-off voltage	9.00	V
Charging method	CC-CV	-

2.5. Simulation Results

A representative result of voltage versus time from the number of simulations is illustrated in Figure 3, and the key parameters such as balancing time and count collected during the corresponding simulation are provided in Table 4. As shown in Figure 3, cell #3 with the highest internal resistance reached the balancing voltage first, as expected [18–23]. As soon as the voltage hit the maximum set voltage, the BMS routine initiated the passive balancing process following the flowchart sequence illustrated in Figure 2. As the balancing process continued its function, the balancing count was traced, monitoring the switching device actions for the connection of the corresponding dissipative balancing circuit. As mentioned earlier, the passive cell balancing processes were performed in the order of the cell with the highest internal resistance first, then, sequentially, down to the cell with the lowest internal resistance. Consequently, the cell with the highest internal resistance generated the highest number of balancing counts. The result of the balancing count for the corresponding simulation is shown in Table 4.

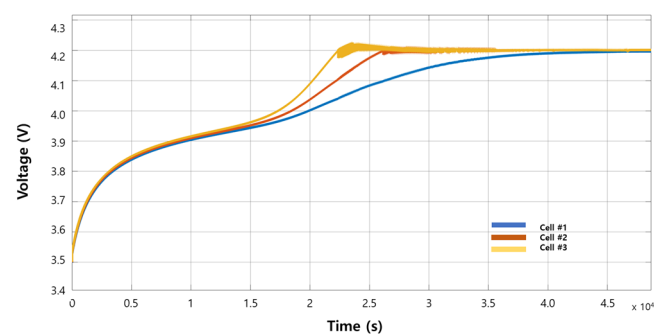


Figure 3. A representative result of cell voltages versus time from a simulation.

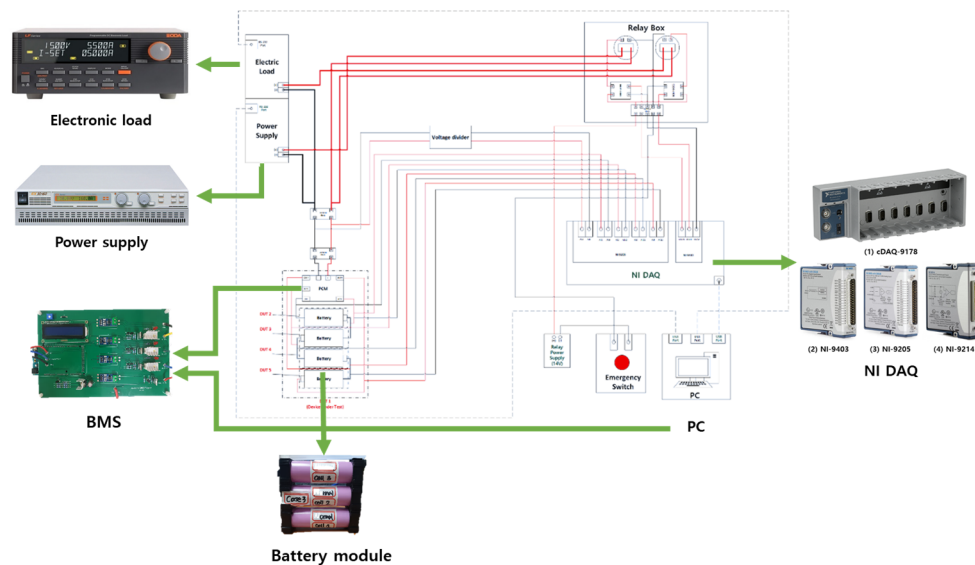
Table 4. Key parameters traced during the corresponding simulation.

Parameter	Cell #1	Cell #2	Cell #3
Balancing time	0	2534	4063
Balancing count	0	198	257

3. Experiments

3.1. Experimental Setup

The experimental setup was designed to go along with the simulation setup shown in Figure 1. A schematic diagram of the overall experimental setup is depicted in Figure 4. In addition, the cell balancing process was programmed following the same algorithm illustrated in Figure 2. Experiments were carried out at an ambient temperature of 25 °C. A battery module of three cells in series was connected to and monitored by a BMS. For the investigation of the behavior of the cell balancing parameters during charging, a programmable power supply was used. The balancing parameters selected to detect faulty cells in the module were measured by the BMS. For convenience, a measurement interval for each balancing parameter was set to one second. Three different battery modules were prepared with different cell combinations, as listed in Table 5. Experiments were conducted using three different modules, where each module consisted of cells with different degradation levels, expecting to obtain reasonably robust results from various configurations, if not perfect. Finally, the BMS used in the experiments was built rather simply to concentrate on the development of the proposed algorithm and the proof-of-concept results, respectively.

**Figure 4.** A schematic diagram of the overall experimental setup.**Table 5.** Battery modules with different cell combinations.

Module	Cell #1	Cell #2	Cell #3
Module #1	Aged	Normal	Normal
Module #2	Normal	Aged	Aged
Module #3	Normal	Normal	Normal

3.2. Experimental Results

The experimental results from the three different modules with difference cell combinations are shown in Figures 5–7. In addition, the balancing time and the balancing count from each cell in the corresponding modules are listed in Tables 6–8. As shown in the figures and tables, the faulty cells with a higher internal resistance compared to the other neighboring cells can be identified quite quickly. For the case of module #1 which consisted of a relatively aged cell #1 and a normal cell #2 and a normal cell #3, the results clearly demonstrate the effectiveness of the proposed algorithm by checking the balancing counts from each cell, as shown in Table 6. Furthermore, tracing the voltage rise among the cells also revealed that the aged cell #1 reached the charging voltage limit faster compared to the other normal cells, as shown in Figure 5. For the case of module #2, which consisted of a normal cell #1 and a relatively aged cell #2 and another relatively aged cell #3, the results effectively show the usefulness of the proposed algorithm by considering the balancing counts, as provided in Table 7. Just as for the case of module #1, by tracing the voltage rise among the cells, it is also revealed that the aged cell #2 and cell #3 reached the charging voltage limit quicker compared to the other normal cell, as shown in Figure 6. Finally, for the case of module #3, which consisted of a normal cell #1, a normal cell #2 and a normal cell #3, the results exhibit somewhat ambiguous results, as expected, due to the cell configuration in module #3. Since the three cells in module #3 are all reasonably normal cells, not like the previous cases, it seems quite normal and expected that none of the balance counts were distinctively notable. Based on the current observations, it is clear that the relatively weaker cell can be quickly identified through the proposed algorithm, which is extremely simple to embed in terms of hardware and software implementation. It is also very valuable to find similar results between the simulations and the experiments. This means that the numerous simulations with different configurations can be executed without too many concerns about the numerical results. The various configurations can certainly include different numbers of cells in series and/or in parallel configurations.

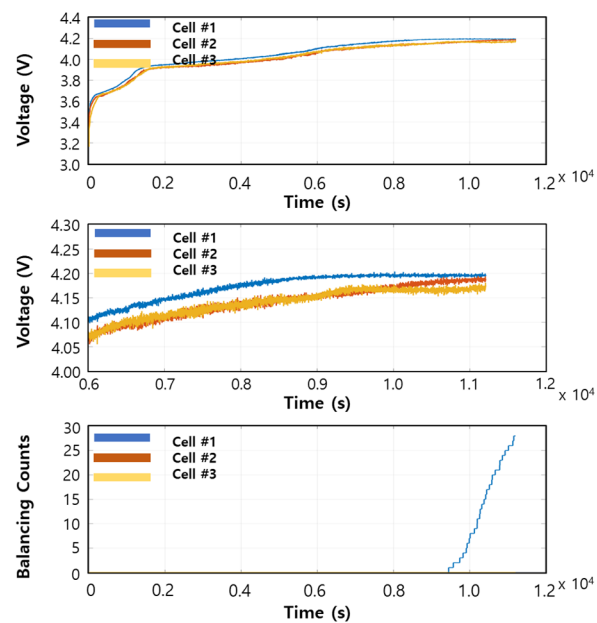


Figure 5. Experimental results from module #1.

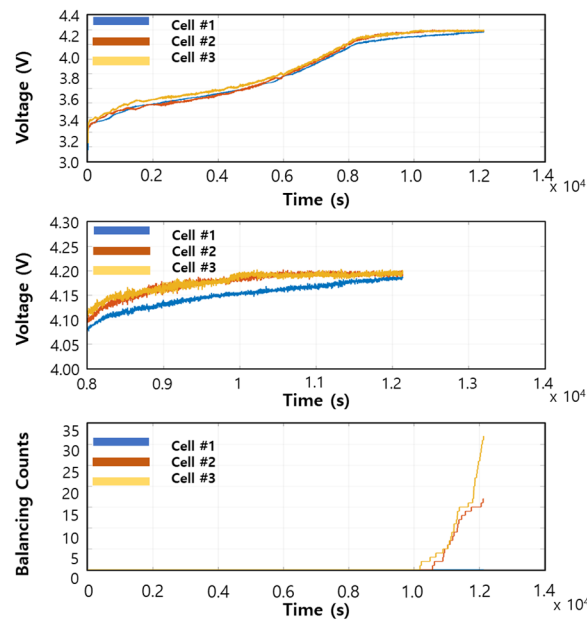


Figure 6. Experimental results from module #2.

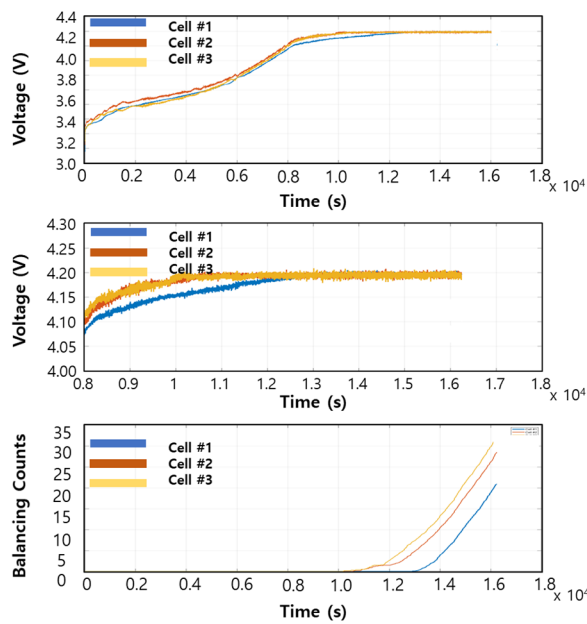


Figure 7. Experimental results from module #3.

Table 6. Balancing parameters from module #1.

Module	Cell #1	Cell #2	Cell #3
Balancing time [s]	1757	0	0
Balancing count	28	0	0

Table 7. Balancing parameters from module #2.

Module	Cell #1	Cell #2	Cell #3
Balancing time [s]	0	1567	1951
Balancing count	0	17	32

Table 8. Balancing parameters from module #3.

Module	Cell #1	Cell #2	Cell #3
Balancing time [s]	3315	5650	6603
Balancing count	209	283	320

4. Discussion

Based on the experimental results, a correlation between the balancing time and the balancing count was analyzed through Equation (1), indicating the Pearson correlation coefficient. $\text{CoV}(X, Y)$ is a covariance of X and Y , which can be expressed as Equation (2), where μ_X and μ_Y are the mean of X and Y , E is an expectation, σ_X is a standard deviation of X and σ_Y is a standard deviation of Y . The Pearson correlation coefficient is a measure of two variables being linearly correlated with each other. If it is close to -1 or 1 , it is determined that there is a strong correlation, and if it is close to 0 , it can be identified as very little or no linear correlation.

$$\rho_{X;Y} = \frac{\text{CoV}(X, Y)}{\sigma_X \sigma_Y} = \frac{\sigma_{XY}}{\sigma_X \sigma_Y}, -1 \leq \rho \leq 1 \quad (1)$$

$$\text{CoV}(X, Y) = E[(X - \mu_X)(Y - \mu_Y)] \quad (2)$$

The Pearson correlation coefficient between balancing counts and balancing time is shown in Table 9, which shows strong correlations for each and every case where the balancing count and the balancing time were obtained. In general, internal resistance is a factor that has a large influence on battery voltage swing during the charging and discharging process [22,23]. Moreover, for the case of a faulty cell typically with yet higher internal resistance, even larger voltage swings are expected than that of normal cells. Thus, it is reasonable to claim that the faulty cells will most likely experience heavier cell balancing processes as they age over and over. Obviously, it becomes critical to monitor this undesirable degradation of cell properties before it reaches the level where it can trigger and propagate the thermal runaway situations. With the proposed faulty cell detection algorithm, it is clear that cells with abnormally high internal resistance can be identified just by monitoring the balancing counts, at least in relative terms, with minimal hardware and software burdens.

Table 9. Correlation coefficient between balancing time and balancing counts.

Module	Correlation Coefficient	Cell #1	Cell #2 Balancing Time	Cell #3
Module #1		0.9932	-	-
Module #2	Balancing counts	-	0.9755	0.9495
Module #3		0.9900	0.9613	0.9694

While the algorithm was initially developed and tested with a proof-of-concept experimental setup, it nicely demonstrated the applicability of the idea. During the conceptual development of the faulty cell detection algorithm, an important assumption was implied. As usually practiced in the manufacturing process, cells are presorted and allocated with similar characteristics, meaning similar internal resistances. Therefore, during the early stage of battery module operations, balancing counts behave just like the case of module #3. However, as cells are recycled over and over, a few cells start to deviate from other neighboring cells. As the degradation becomes more obvious, the proposed detection algorithm can set off the alarm signal for the system level response to take care of the dangerous situations accordingly.

5. Conclusions

In this paper, a simple and straightforward faulty cell detection algorithm was proposed to enhance the safe operation of lithium-ion battery modules/packs. As illustrated in the paper, the algorithm implementation was quite simple and required very little hardware and software resources. The simulation results and the experimental results confirm the applicability of the algorithm in the actual BMS with very little resource burdens. Through the current study, the faulty cell detection algorithm based on the balancing count can be used as an additional indicator to enhance the safety of lithium-ion battery modules/packs. Moreover, it is very important to note that the battery cells with increased internal resistance can be detected by using balancing tracking, even without temperature sensors.

In order to further develop and improve the algorithm, BMS hardware with 12 cells in series and three strings in parallel configuration is being prepared. Simulation models are ready and the preliminary results from the simulation show quite promising outcomes. As soon as the BMS is ready and the data become available, another research report will be submitted to the journal.

Author Contributions: Conceptualization, W.C.; methodology, W.C.; validation, W.C. and S.H.; formal analysis, S.H.; resources, S.H.; writing—original draft preparation, S.H.; writing—review and editing, W.C. All authors have read and agreed to the published version of the manuscript.

Funding: This research received no external funding.

Institutional Review Board Statement: Not applicable.

Informed Consent Statement: Not applicable.

Data Availability Statement: Not applicable.

Conflicts of Interest: The authors declare no conflict of interest.

References

1. Yang, Y.; Bremner, S.; Menictas, C.; Merlinda, K. Battery energy storage system size determination in renewable energy systems: A review. *Renew. Sustain. Energy Rev.* **2018**, *91*, 109–125. [[CrossRef](#)]
2. Pelegov, D.; Pontas, J. Main drivers of battery industry changes: Electric vehicles—A market overview. *Batteries* **2018**, *4*, 65. [[CrossRef](#)]
3. Chen, W.; Liang, J.; Yang, Z.; Li, G. A review of lithium-ion battery for electric vehicle applications and beyond. *Energy Procedia* **2019**, *158*, 4363–4368. [[CrossRef](#)]
4. Hansen, J.F.; Wendt, F. History and state of the art in commercial electric ship propulsion, integrated power systems, and future trends. *Proc. IEEE* **2015**, *103*, 2229–2242. [[CrossRef](#)]
5. Zhang, C.; Wei, Y.L.; Cao, P.F.; Lin, M.C. Energy storage system: Current studies on batteries and power condition system. *Renew. Sustain. Energy Rev.* **2018**, *82*, 3091–3106. [[CrossRef](#)]
6. Lawder, M.T.; Suthar, B.; Northrop, P.W.; De, S.; Hoff, C.M.; Leitermann, O.; Subramanian, V.R. Battery energy storage system (BESS) and battery management system (BMS) for grid-scale applications. *Proc. IEEE* **2014**, *102*, 1014–1030. [[CrossRef](#)]
7. Rahimi-Eichi, H.; Ojha, U.; Baronti, F.; Chow, M.Y. Battery management system: An overview of its application in the smart grid and electric vehicles. *IEEE Ind. Electr. Mag.* **2013**, *7*, 4–16. [[CrossRef](#)]
8. Hannan, A.M.; Hoque, M.M.; Hussain, A.; Yusof, Y.; Ker, P.J. State-of-the-art and energy management system of lithium-ion batteries in electric vehicle applications: Issues and recommendations. *IEEE Access* **2018**, *6*, 19362–19378. [[CrossRef](#)]
9. Kim, Y.; Samad, N.A.; Oh, K.Y.; Siegel, J.B.; Epureanu, B.I.; Stefanopoulou, A.G. Estimating state-of-charge imbalance of batteries using force measurements. In Proceedings of the 2016 American Control Conference (ACC), Boston, MA, USA, 6–8 July 2016; pp. 1500–1505.
10. Lin, X.; Stefanopoulou, A.G.; Li, Y.; Anderson, R.D. State of charge imbalance estimation for battery strings under reduced voltage sensing. *IEEE Trans. Control. Syst. Technol.* **2014**, *23*, 1052–1062.
11. Liu, K.; Li, K.; Peng, Q.; Zhang, C. A brief review on key technologies in the battery management system of electric vehicles. *Front. Mech. Eng.* **2019**, *14*, 47–64. [[CrossRef](#)]
12. Yildirim, B.; Elgendy, M.; Smith, A.; Pickert, V. Evaluation and Comparison of Battery Cell Balancing Methods. In Proceedings of the 2019 IEEE PES Innovative Smart Grid Technologies Europe (ISGT-Europe), Bucharest, Romania, 29 September–2 October 2019; pp. 1–5.
13. Aizpuru, I.; Iraola, U.; Canales, J.M.; Echeverria, M.; Gil, I. Passive balancing design for Li-ion battery packs based on single cell experimental tests for a CCCV charging mode. In Proceedings of the 2013 International Conference on Clean Electrical Power (ICCEP), Alghero, Italy, 11–13 June 2013; pp. 93–98.

14. Amin; Ismail, K.; Nugroho, A.; Kaleg, S. Passive balancing battery management system using MOSFET internal resistance as balancing resistor. In Proceedings of the 2017 International Conference on Sustainable Energy Engineering and Application (ICSEEA), Jakarta, Indonesia, 23–26 October 2017; pp. 151–155.
15. Docimo, D.J.; Fathy, H.K. Analysis and control of charge and temperature imbalance within a lithium-ion battery pack. *IEEE Trans. Control. Syst. Technol.* **2018**, *27*, 1622–1635. [[CrossRef](#)]
16. Xiong, R.; Pan, Y.; Shen, W.; Li, H.; Sun, F. Lithium-ion battery aging mechanisms and diagnosis method for automotive applications: Recent advances and perspectives. *Renew. Sustain. Energy Rev.* **2020**, *131*, 110048. [[CrossRef](#)]
17. Barré, A.; Deguilhem, B.; Grolleau, S.; Gérard, M.; Suard, F.; Riu, D. A review on lithium-ion battery ageing mechanisms and estimations for automotive applications. *J. Power Sources* **2013**, *241*, 680–689. [[CrossRef](#)]
18. Kobayashi, Y.; Kobayashi, T.; Shono, K.; Ohno, Y.; Mita, Y.; Miyashiro, H. Decrease in capacity in Mn-based/graphite commercial lithium-ion batteries: I. Imbalance proof of electrode operation capacities by cell disassembly. *J. Electrochem. Soc.* **2013**, *160*, A1181. [[CrossRef](#)]
19. Anseán, D.; García, V.M.; González, M.; Blanco-Viejo, C.; Viera, J.C.; Pulido, Y.F.; Sánchez, L. Lithium-ion battery degradation indicators via incremental capacity analysis. *IEEE Trans. Ind. Appl.* **2019**, *55*, 2992–3002. [[CrossRef](#)]
20. Zhang, D.; Haran, B.S.; Durairajan, A.; White, R.E.; Podrazhansky, Y.; Popov, B.N. Studies on capacity fade of lithium-ion batteries. *J. Power Sources* **2000**, *91*, 122–129. [[CrossRef](#)]
21. Tröltzsch, U.; Kanoun, O.; Tränkler, H.R. Characterizing aging effects of lithium ion batteries by impedance spectroscopy. *Electrochim. Acta* **2006**, *51*, 1664–1672. [[CrossRef](#)]
22. Osaka, T.; Nakade, S.; Rajamäki, M.; Momma, T. Influence of capacity fading on commercial lithium-ion battery impedance. *J. Power Sources* **2003**, *119*, 929–933. [[CrossRef](#)]
23. Gantenbein, S.; Schönleber, M.; Weiss, M.; Ivers-Tiffée, E. Capacity fade in lithium-ion batteries and cyclic aging over various state-of-charge ranges. *Sustainability* **2019**, *11*, 6697. [[CrossRef](#)]